DALTON
FULL PAPER

The binding of Ni(II) and Cu(II) with the N-terminal tail of the histone H4

Maria Antonietta Zoroddu,*[a] Massimiliano Peana,[a] Teresa Kowalik-Jankowska,[b] Henryk Kozłowski[b] and Max Costa[c]

[a] *Department of Chemistry, University of Sassari, Via Vienna 2, 07100 Sassari, Italy. E-mail: zoroddu@uniss.it*
[b] *Faculty of Chemistry, University of Wroclaw, Poland*
[c] *Department of Environmental Medicine, New York University, School of Medicine, NY, USA*

Received 12th June 2001, Accepted 22nd October 2001
First published as an Advance Article on the web 16th January 2002

We have analyzed, for Ni(II) and Cu(II) binding, the sequence of the N-terminal tail of the histone H4, the 22-amino acid peptide Ac-SGRGKGGKGLGKGGAKRHRKVL-Am and, in addition, the 7- and 11-amino acid peptides Ac-AK(Ac)RHRK(Ac)V-Am, Ac-GK(Ac)GGAK(Ac)RHRK(Ac)V-Am where all side chains of lysines were blocked by acetylation. Potentiometric and spectroscopic studies (UV-Vis, CD, EPR, NMR) showed that histidine 18 acted as an anchoring binding site for metal ions in all the peptides investigated. The stability constants of the 3N and 4N complexes are higher than those obtained for simple peptides with glycine instead of arginine and lysine residues in the metal binding site. The coordination was not significantly affected by the acetylation of lysines.

The behavior of the "tail" suggested a possible bent structure with organized side-chain orientation promoted by Ni(II).

Introduction

Nickel compounds are known human carcinogens.[1] The molecular mechanism of nickel carcinogenicity, though not fully understood, is believed to involve DNA damage and epigenetic effects in chromatin resulting from nickel binding inside the cell nucleus.[2–4] It is known that DNA and phospholipids of cellular membranes do not provide binding sites of high affinity for Ni^{2+}.[5] Consequently, the nuclear proteins, and in particular the most abundant among them, the histones, reaching in somatic cells formal concentration of 3 mM, are able to compete for metal ions with even higher affinity metal binding sites in other less abundant nuclear proteins or smaller molecules. Fagocytosis of insoluble particles of Ni_3S_2 by either macrophages or epithelial cells causes build-up of very high levels of nickel inside the cells after its intracellular dissolution catalyzed by the acidic pH of endocytic vacuoles, then providing a continuous source of Ni(II) ions. The carcinogenic potency of Ni(II) compounds is related to the ability of Ni(II) to access chromatin, where it produces an increased chromatin condensation, enhances DNA methylation, and turns off the transcription of tumor suppressor and senescence genes. We have previously reported[6,7] that N-terminal tails of core histones are sites for post-translational modifications such as the acetylation involved in nickel toxicity. The sites of acetylation are the lysine residues of the positively charged amino terminal tails of H4. The positive charge of the H4 tail is neutralized by acetylation at lysines 5, 8, 12 and 16, increasing the access to transcription factors and making "active chromatin" more available for modifications.[8]

It has been proposed that the binding of Ni(II) ions within the cell nucleus is a crucial element in the mechanism of carcinogenesis. The detection and structural and mechanistic description of specific Ni(II) sites in histones would provide a molecular basis for better understanding of the mechanisms underlying Ni(II)-induced carcinogenesis.

This prompted us to examine, in addition to the structural data of nucleosome core particles, the amino acid sequences of histones in order to identify potential Ni(II) binding motifs. Available information on the binding modes of Ni(II) to proteins and data for nickel-peptide complexes indicate that the imidazole of histidine and thiol of cysteine should be thermodynamically preferred by Ni(II) among the donor groups provided by protein-building amino acid. Carboxyl groups of aspartate and glutamate can play only secondary roles in the binding. The search for potential nickel binding sites in the histones should therefore be focused on terminal sequences, histidine and cysteine.

Using this information, we inspected amino acid sequences of histones. H1 does not have any histidine or cysteine residues. Inspection of the available histone sequences revealed several histidine and cysteine residues in H2, H3 and H4.

Looking at the X-ray crystal structure of the nucleosome core particle, histidine and cysteine residues in H2 and H3 histones are located inside the molecule in the protein interior. The amino termini of histones extend, on the contrary, out from the core where they are accessible (and can be *post-translationally* modified by acetylation). A histidine (His 18) can be seen in the mobile N-terminal tail of the histone H4. It is one of the most conserved proteins in nature, even for the amino terminal region (residues 1–22) which features three repetitions of the sequence Gly–Lys–Gly and the unusual string of five basic residues –KRHRK– (–Lys–Arg–His–Arg–Lys–) which may serve as a binding locus for anionic modifiers of histone protein tertiary structure or for selectively binding nucleic acid. Therefore, our attention has been focused on the N-terminal tail of H4 and the 22-amino acid sequence of the tail has been selected as a candidate for specific binding site in the octamer.

Here we report the interaction of Ni(II) with the sequence of the N-terminal tail of H4, the 22-amino acid peptide Ac-SGRGKGGKGLGKGGAKRHRKVL-Am (peptide 1), where all sites for post-translational modification involved in nickel and in copper toxicity have been included.

The binding study was also extended to copper in view of the reported toxicity of this metal as a novel inhibitor of H4

 DOI: 10.1039/b105128h

acetylation on the lysines close to histidine 18 in the N-terminal tail of H4[7] and also to investigate if subtle differences in the coordination behavior can result in different toxicological activity.

A comparison of the binding capabilities of the simple motif AKRHRK with the 7-amino acid Ac-AK(Ac)RHRK(Ac)V-Am (peptide 2) and 11-amino acid Ac-GK(Ac)GGAK(Ac)-RHRK(Ac)V-Am (peptide 3) where all side chains of lysines have been acetylated, is also reported.

To make the tail and the two shorter peptides more relevant models of the H4 protein, the C-terminus for peptide 1 was blocked by amidation and the N- and C- for peptides 2 and 3 were blocked by acetylation and amidation.

Experimental

Peptide synthesis

Ac-SGRGKGGKGLGKGGAKRHRKVL-Am (peptide 1), Ac-AK(Ac)RHRK(Ac)V-Am (peptide 2) and Ac-GK(Ac)-GGAK(Ac)RHRK(Ac)V-Am (peptide 3) peptide sequences were synthesized on a solid support with a 9050 Plus Synthesizer by BBM Inc. (Woburn, MA) using a conventional Fmoc chemistry methodology[9] starting from the carboxy terminal to the amino terminal. N-Fmoc protected amino acids and all other peptide synthesis reagents were obtained from PE Biosystem, USA. The peptide was purified using semipreparative HPLC on a C_{18} column eluting with 0.1% CF_3COOH–H_2O (solvent A) and 0.1% CF_3COOH–CH_3CN (solvent B), linear gradient 0–100% B over 50′ at a 3 ml min^{-1} flow rate with 220 nm absorption used as a means of detection. The purity of the peptide was checked by reversed phase HPLC using a C_{18} 5 μm 100A microsorb-MV analytical column; 4.6 mm × 25 cm, flow rate 1 ml min^{-1}, gradient 0–50% in 25′ (solvent A), 50–100% in 35′ (solvent B). The molecular weight of the peptide was confirmed by mass spectral analysis (MALDI.TOF.VOYAGER).

Potentiometric measurements

Stability constants for protons, copper(II) and nickel(II) complexes were calculated from titration curves carried out at 25 °C. The total volume of the resultant solution used for the titration experiments was 1.5 cm^3. NaOH (10^{-3} M) was added from a 0.250 cm^3 micrometer syringe which was calibrated by both weight titration and the titration of standard materials. Metal ion concentration was 1.5×10^{-3} mol dm^{-3} and the metal-to-ligand molar ratio was 1 : 1.1. The pH-metric titrations were performed at 25 °C in 0.10 mol dm^{-3} KNO_3 on a MOLSPIN pH-meter system using a Russel CMAW 711 microcombined electrode calibrated in hydrogen ion concentrations using HNO_3.[10] The SUPERQUAD computer program was used for stability constant calculations.[11] Standard deviations quoted were computed by SUPERQUAD, and refer to random errors only. They are, however, a good indication of the importance of a particular species in the equilibrium.

For Ac-GK(Ac)GGAK(Ac)RHRK(Ac)V-Am (peptide 3) it was not possible to perform the potentiometric measurements because of hydrolysis with raising the pH. In this case only spectroscopic measurements were carried out.

Spectroscopic measurements

Solutions were of similar concentrations to those used in the potentiometric studies for EPR, CD and UV-Vis measurements. EPR spectra were recorded on a Bruker ESP 300E and a Varian E-9 spectrometer at X-band frequency at 120 K. The EPR parameters were calculated for the spectra obtained at the maximum concentration of the particular species for which well-resolved separations were observed. Absorption spectra were recorded on a Beckman DU 650 spectrophotometer. Circular dichroism (CD) spectra were recorded on a Jasco J 600 spectropolarimeter in the 750–250 nm range. The values of $\Delta\varepsilon$ (*i.e.*, $\varepsilon_l - \varepsilon_r$) and ε were calculated at the maximum concentration of the particular species obtained from the potentiometric data.

NMR experiments were performed on a Varian 300-VXR spectrometer.[12] The 1D experiments were carried out in D_2O solutions at a peptide concentration of 2 mM and peptide : Ni(II) ratio of 1.1 : 1 in the pH range 9 to 11 for peptides 1 and 2 (the pH* reading of the electrode was not corrected for the isotope effect). pH* was adjusted with 2 M NaOH and monitored on an Aldrich extra long stem electrode inside the NMR tubes.

Results

Protonation constants

The potentiometrically measured protonation constants are shown in Table 1 along with the calculated stepwise constants assigned to the respective peptidic functions. For comparison, in Table 1 the protonation constants are reported for the N- and C-blocked peptides containing the histidine residue.[6,13–16]

The 22-amino acid sequence (peptide 1) can be considered as an H_6L ligand where the deprotonation involves the histidine residue (pK = 5.99) and the five side chains of the lysine residues (pK = 11.79, 10.75, 10.08, 10.03 and 9.20, Table 1). The 7-amino acid peptide (Ac-AK(Ac)RHRK(Ac)V-Am, peptide 2) is an HL ligand where the deprotonation involves the histidine residue (pK = 6.08). As we can see from the values of the pK_a reported in Table 1, the imidazole nitrogens of the histidine residues for both peptides investigated, the tail of the H4 (peptide 1) and the heptapeptide (peptide 2), are about one order of magnitude more acidic than the histidine in the Boc-AGGH peptide or Ac-GGGH.

Potentiometry detects a range of Ni(II) and Cu(II) complexes with the formation constants reported in Tables 2 and 3 respectively. The values of log K* are the protonation corrected stability constants which are useful to compare the ability of various ligands to bind a metal ion.[17,18] Spectroscopic properties of major complexes are given in Table 4.

Ni(II) complexes

Histidine residues can be a primary binding site for Ni(II) ions in the histone core of the nucleosome. Therefore, the H4 tail can potentially be one of the biologically relevant sites for nickel genotoxicity. The coordination ability of the entire tail towards Ni(II) is similar to that found previously for the hexapeptide fragment AKRHRK,[6] therefore, His 18 acted as an anchoring binding site for nickel ions in the entire tail of the histone H4.

Ni(II) forms eight complex species with the 22-amino acid peptide 1 (Table 2), from the minor octahedral NiH_4L (a 2N complex) and NiH_3L (a 3N complex) up to the six square planar 4N species: NiH_2L, NiHL, NiL $NiH_{-1}L$, $NiH_{-2}L$, $NiH_{-3}L$ species (Fig. 1(a)). The latter six species differ by the number of protonated Lys residues. The consecutive deprotonations of the side chains of five lysine residues takes place with pK values 11.2, 10.62, 10.16, 9.98 and 9.19. Above pH 9.5 three 4N species NiH_2L, NiHL and NiL account for about 90-% of the total metal present. The absorption and CD spectra of the latter complexes are typical for 4N planar diamagnetic complexes.[19–21] The spectroscopic data are reported in Table 4.

Four species were obtained for peptide 2: NiL, $NiH_{-1}L$, $NiH_{-3}L$ and $NiH_{-4}L$ (Fig. 1(b)). The coordination behavior is similar to that observed for the motifs where lysines are free. In the species $NiH_{-4}L$ the deprotonation of the pyrrolic nitrogen takes place.

The behavior of Ac-GK(Ac)GGAK(Ac)RHRK(Ac)V-Am (peptide 3) is the same as the 7-amino acid peptide 2, giving the

Table 1 Protonation constants for Ac-SGRGKGGKGLGKGGAKRHRKVL-Am (**peptide 1**), Ac-AK(Ac)RHRK(Ac)V-Am (**peptide 2**) and comparable peptide at 298 K, $I = 0.1$ M (KNO_3)

	log β/species							
	HL	H_2L	H_3L	H_4L	H_5L	H_6L	H_7L	H_8L
peptide 1	**11.79 ± 0.10**	**22.54 ± 0.06**	**32.62 ± 0.09**	**42.65 ± 0.07**	**51.85 ± 0.08**	**57.84 ± 0.08**		
peptide 2	**6.08 + 0.01**							
Ac-AKRHRK-Am[a]	11.03	20.90	27.03					
Ac-EVRHQK-Am[b]	10.19	16.45	20.49					
Ac-DAEFRH-Am[c]	6.50	10.95	14.45					
Ac-DAEFGH-Am[c]	6.79	11.39	15.02					
Boc-AGGH[d]	7.19	10.02						
Cap43[e]	6.35	10.36						
Ac-GGGH[f]	7.21							

Stepwise protonation constants

	log K								
	NH_{2Lys}	NH_{2Lys}	NH_{2Lys}	NH_{2Lys}	NH_{2Lys}	NH_2	N_{Im}	COO^-	COO^-
peptide 1	**11.79**	**10.75**	**10.08**	**10.03**	**9.20**		**5.99**		
peptide 2							**6.08**		
Ac-AKRHRK-Am	11.03	9.87					6.13		
Ac-EVRHQK-Am	10.19						6.26	4.04	
Ac-DAEFRH-Am							6.50	4.45	3.50
Ac-DAEFGH-Am							6.79	4.60	3.63
Boc-AGGH							7.19	2.83	
Cap43							6.35	4.01	
Ac-GGGH							7.21	3.16	

[a] Ref. 6. [b] Ref. 13. [c] Ref. 14. [d] Ref. 15. [e] Ref. 16. [f] Ref. 23.

Table 2 Stability constants of N(II) complexes with Ac-SGRGKGGKGLGKGGAKRHRKVL-Am (**peptide 1**), Ac-AK(Ac)RHRK(Ac)V-Am (**peptide 2**) and comparable peptides at 298 K and $I = 0.10$ M (KNO_3)

	log β/species								
	NiH_4L	NiH_3L	NiH_2L	NiHL	NiL	$NiH_{-1}L$	$NiH_{-2}L$	$NiH_{-3}L$	$NiH_{-4}L$
peptide 1	**45.50 ± 0.05**	**37.15 ± 0.06**	**29.17 ± 0.01**	**19.98 ± 0.01**	**10.00 ± 0.02**	**−0.16 ± 0.02**	**−10.78 ± 0.02**	**−21.98 ± 0.02**	
peptide 2					**2.62 ± 0.06**	**−5.34 ± 0.05**		**−22.12 ± 0.03**	**−33.37 ± 0.01**
Ac-AKRHRK-Am[a]			23.01	15.05		−1.67	−11.80	−22.84	
Cap43[b]					2.73		−13.47	−21.81	
Boc-AGGH[c]						−4.49		−22.83	

	log K*			
	1N	2N	3N	4N
peptide 1		**−12.34**	**−20.69**	**−28.67**
peptide 2	**−3.46**	**−11.42**		**−28.20**
Ac-AKRHRK-Am	−4.02	−11.98		−28.70
Cap43	−3.62		−19.82	−28.16
Boc-AGGH		−11.68		−30.02

	Values for ionization of the first, second and third amide groups		
	pK_1(amide)	pK_2(amide)	pK_3(amide)
peptide 1		**8.35**	**7.98**
peptide 2	**7.96**		
Ac-AKRHRK-Am	7.96		
Cap43			8.34

[a] Ref. 6. [b] Ref. 16. [c] Ref. 15. log K* = log $\beta(NiH_jL)$ − log $\beta(H_nL)$ ($j = 4, 3, 2$ and $n = 6$ for peptide 1; $j = 0, -1, -3$ and $n = 1$ for peptide 2).

same spectroscopic results. The UV-Vis spectra with changing pH are reported in Fig. 2.

The log K* values for the 4N complexes of the ligands studied here are comparable to those found for Ac-AKRHRK-Am[6] and Cap43 (Ac-TRSRSHTSEGTRSR-Am sequence)[16] peptides, but they are higher by about 1.5 orders of magnitude than that for the Boc-AGGH peptide (Table 2).

^{1}H NMR spectra of D_2O solutions containing peptide 1 and peptide 2 were studied over the pH range 9–11 and assignments for free ligands and diamagnetic 4N species were performed by 1D experiments. Aromatic regions of the NMR spectra are reported in Fig. 3. It is clear that some free peptide was still present in the solution of Ni–N4–"tail" species. The ratio of free to bound peptide appeared to be 1 : 4 on the basis of

Table 3 Stability constants of Cu(II) complexes of Ac-SGRGKGGKGLGKGGAKRHRKVL-Am (**peptide 1**), Ac-AK(Ac)RHRK(Ac)V-Am (**peptide 2**) and comparable peptide at 298 K and $I = 0.10$ M (KNO_3)

	log β/species									
	CuH_5L	CuH_4L	CuH_3L	CuH_2L	CuHL	CuL	$CuH_{-1}L$	$CuH_{-2}L$	$CuH_{-3}L$	$CuH_{-4}L$
peptide 1	**55.16 ± 0.02**	**49.38 ± 0.01**	**43.88 ± 0.01**	**36.05 ± 0.01**	**26.99 ± 0.01**	**17.13 ± 0.01**	**7.03 ± 0.02**	**−3.54 ± 0.02**	**−14.71 ± 0.02**	
peptide 2						**3.33 ± 0.03**	**−2.77 ± 0.04**	**−8.23 ± 0.01**	**−16.53 ± 0.01**	**−27.29 ± 0.03**
Ac-AKRHRK-Am[a]				23.70		12.45	3.98	−5.94	−16.92	
Ac-EVRHQK-Am[b]					14.01		1.93	−6.66	−16.83	
Ac-DAEFRH-Am[c]						4.49		−8.14	−16.16	
Ac-DAEFGH-Am[c]						4.95	−2.23	−8.48	−15.91	
Cap43[d]						4.26	−1.72	−7.56	−15.04	

	log K*			
	1N	2N	3N	4N
peptide 1	**−2.68**	**−8.46**	**−13.96**	**−21.79**
peptide 2	**−2.75**	**−8.85**	**−14.31**	**−22.61**
Ac-AKRHRK-Am	−3.33		−14.58	−23.05
Ac-EVRHQK-Am	−2.44		−14.52	−23.11
Ac-DAEFRH-Am	−2.01		−14.64	−22.66
Ac-DAEFGH-Am	−1.84	−9.02	−15.27	−22.70
Cap43	−2.09	−8.07	−13.91	−21.39

	Values for ionization of the first, second and third amide groups		
	pK_1(amide)	pK_2(amide)	pK_3(amide)
peptide 1	**5.78**	**5.50**	**7.83**
peptide 2	**6.10**	**5.46**	**8.30**
Ac-AKRHRK-Am			8.47
Boc-AGGH	6.79	6.67	8.93
Ac-GGGH[e]	6.50	7.35	8.80
Ac-EVRHQK-Am			8.59
Ac-DAEFRH-Am			8.02
Ac-DAEFGH-Am	7.18	6.25	7.43
Cap43	5.98	5.84	7.48

[a] Ref. 6. [b] Ref. 13. [c] Ref. 14. [d] Ref. 15. [e] Ref. 23. $\log K^* = \log \beta(CuH_jL) - \log \beta(H_nL)$ ($j = 5, 4, 3, 2$ and $n = 6$ for peptide 1, $j = 0, -1, -2, -3$ and $n = 1$ for peptide 2).

Table 4 Spectroscopic data for the copper(II) and nickel(II) complexes of Ac-SGRGKGGKGLGKGGAKRHRKVL-Am (**peptide 1**), Ac-AK(Ac)RHRK(Ac)V-Am (**peptide 2**)

	Absorption		CD		EPR	
Species	λ/nm	$(\varepsilon)^a$	λ/nm	$(\Delta\varepsilon)$	$A_{//}$	$g_{//}$/G
Cu^{2+} complexes						
peptide 1						
CuH_3L (3N)	601 [b]	72	538	+0.448 [b]	167	2.226
			339	−0.568 [c,d]		
CuH_2L (4N)	515 [b]	106	629	+0.764 [b]	200	2.185
			490	−0.789 [b]		
			356	−0.148 [c]		
			315	+0.826 [d]		
CuHL, CuL (4N)	517 [b]	120	633	+0.747 [b]	205	2.187
$CuH_{-1}L$, $CuH_{-2}L$ (4N)			490	−0.806 [b]		
$CuH_{-3}L$ (4N)			356	−0.127 [c]		
			315	+0.808 [d]		
peptide 2						
$CuH_{-2}L$ (3N)	597 [b]	64	531	+0.344 [b]	167	2.230
			342	−0.545 [c]		
$CuH_{-3}L$ (4N)	516 [b]	90	640	+0.720 [b]	200	2.188
			491	−1.289 [b]		
			357	−0.150 [c]		
			315	+0.719 [d]		
peptide 3						
pH 6.5–7.5 (3N)	602	66	536	+0.358	167	2.230
			635	+0.872		
			487	−1.332		
			357	−0.202		
			315	+0.981		
from pH 9.5 (4N)	513	90			197	2.189
Ni^{2+} complexes						
peptide 1						
NiH_2 L (4N)	437 [b]	199	516	+0.845 [b]		
	485 [b] sh	134	423	−2.646 [b]		
NiHL, NiL (4N)	439 [b]	204	516	+0.797 [b]		
$NiH_{-1}L$, $NiH_{-2}L$ (4N)	487 [b] sh	128	423	−2.617 [b]		
$NiH_{-3}L$ (4N)						
peptide 2						
$NiH_{-3}L$ (4N)	439 [b]	104	513	+0.512 [b]		
	494 [b] sh	74	420	−1.485 [b]		
peptide 3						
from pH 8 (4N)	440	101	513	+1.052		
			422	−2.625		

[a] From the visible and CD results, M^{-1} cm^{-1}. [b] d–d transition. [c] $N_{imidazole} \Rightarrow Cu^{2+}$ charge transfer transition. [d] $N^-_{amide} \Rightarrow Cu^{2+}$ charge transfer transition.

integrals. The differential broadening of resonances were the most striking features. They provide an indication of the location of nickel binding in the tail, which can be assigned towards the N-terminal of the tail.

The proton NMR spectra showed significant downfield and upfield changes, particularly within the αCH proton region as a result of complexation of Ni(II) to the H4 tail. The shift of the two histidine aromatic protons from 7.63 to 7.539 and from 6.883 to 6.796 ppm for peptide 1 at pH 9.5 was indicative of the involvement of the imidazolic nitrogen in the coordination. A shift of the α and β protons of histidine from 4.5 to 4.36 and from 2.983 to 2.907 ppm was observed.

Cu(II) complexes

The stability constants and stoichiometry of the complexes obtained from the potentiometric data calculations are given in Table 3. CuH_3L (a 3N species) was the major complex found from pH 5 to pH 7.5. At pH 8.2 the major complex is a 4N species, CuH_2L, involving the imidazole nitrogen and three nitrogens from deprotonated amides from the backbone of the peptide (Fig. 4). The spectroscopic parameters of the species are reported in Table 4. The CuH_3L complex with a d–d transition at 601–597 nm (absorption spectra), the presence in the CD spectra of the $N_{Im} \longrightarrow Cu^{2+}$ charge transfer transition at 342–339 nm and EPR parameters $A_{\parallel} = 167$ G, $g_{\parallel} =$ 2.226–2.230 suggest the 3N complex with $\{N_{Im}, 2N^-_{amide}\}$ coordination mode (13–14, 24–25). Similar EPR parameters were observed earlier for the 3N coordination with $\{N_{Im}, 2N^-_{amide}\}$ binding mode.[6,13,16] The low values of $A_{\parallel}$ obtained for these complexes may suggest distortion of the tetragonal geometry around the metal ion. That the copper site is not exactly axial is also seen in the perpendicular region of the EPR spectrum. The increase in the total number of superhyperfine lines, greater than that expected for three coordinated nitrogen atoms, can result from a small separation between g_x and g_y

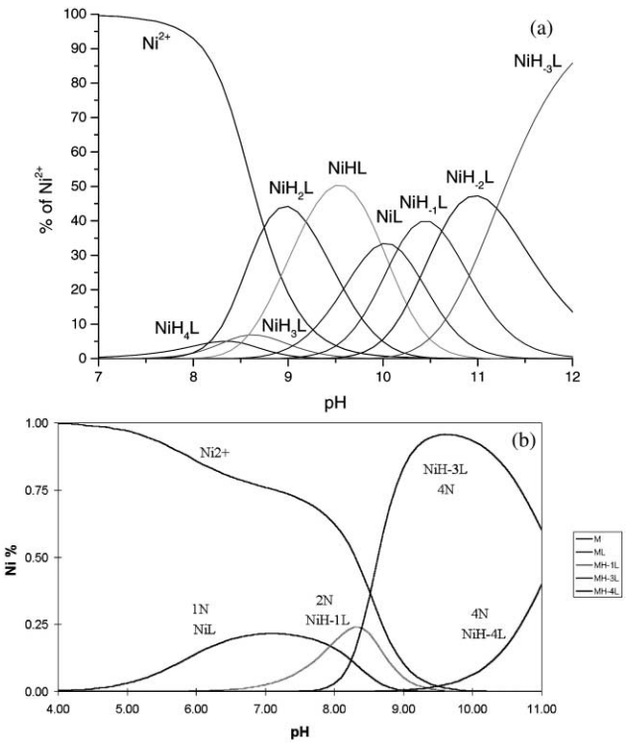

Fig. 1 Species distribution curves for Ni^{2+} complexes of (a) Ac-SGRGKGGKGLGKGGAKRHRKVL-Am (peptide 1). (b) Ac-AK-(Ac)RHRK(Ac)V-Am (peptide 2). Ni^{2+}-to-peptide molar ratio 1 : 1, $[Ni^{II}] = 0.001$ M.

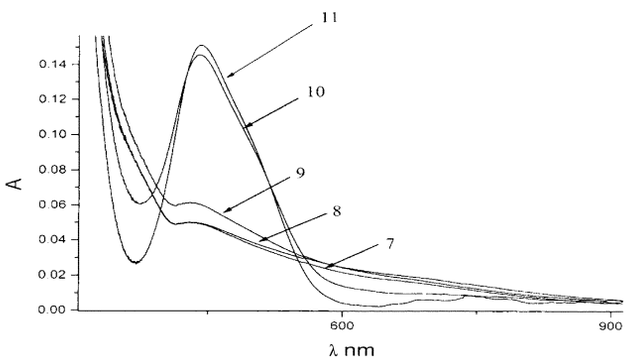

Fig. 2 UV-Vis spectra of Ac-AK(Ac)RHRK(Ac)V-Am–Ni(II) system with changing pH.

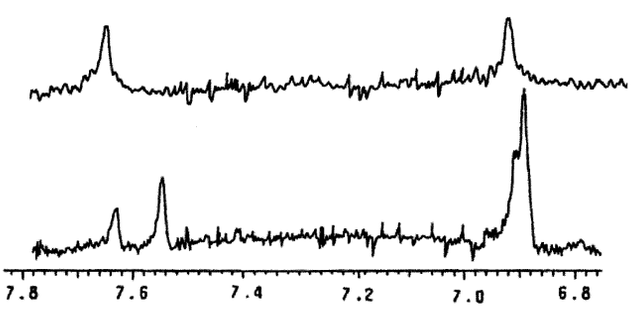

Fig. 3 NMR aromatic region of (upper curve) Ac-SGRGKGGKGL-GKGGAKRHRKVL-Am–peptide and (lower curve) Ac-SGRGKG-GKGLGKGGAKRHRKVL-Am–Ni(II) at pH = 9.5.

allowing superhyperfine lines to appear on each feature (Fig. 5(a)).

Above pH 6, the deprotonation of the amide proton in both studied systems occurs and the 4N complexes are formed. The shift of the d–d transition towards 515–516 nm, EPR parameters $A_{||} = 200$–205 G, $g_{||} = 2.185$–2.187 and the presence in the CD spectra of the $N_{Im} \longrightarrow Cu(II)$ and $N^-_{amide} \longrightarrow$

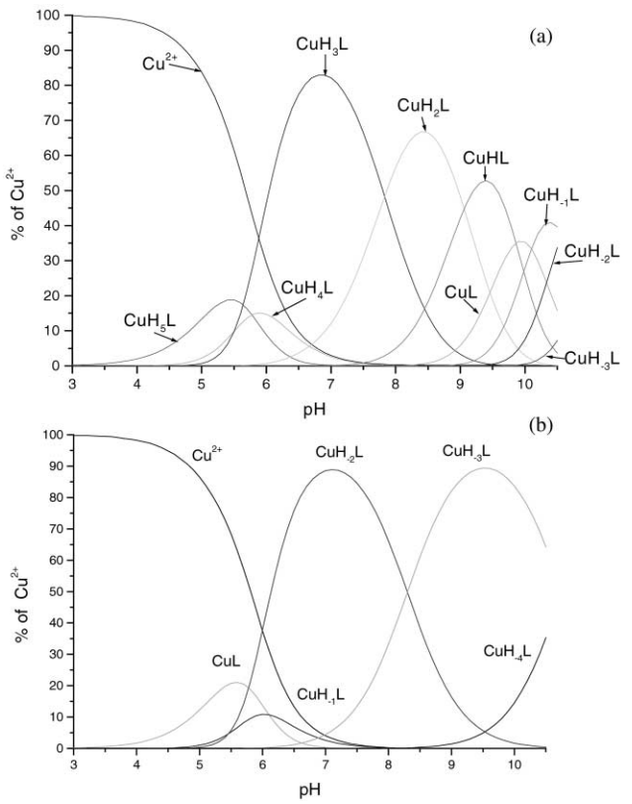

Fig. 4 Species distribution curves for Cu(II) complexes of (a) Ac-SGRGKGGKGLGKGGAKRHRKVL-Am (peptide 1). (b) Ac-AK-(Ac)RHRK(Ac)V-Am (peptide 2). Cu^{2+}-to-peptide molar ratio 1 : 1, $[Cu^{II}] = 0.001$ M.

Cu(II) charge transfer transitions support this suggestion and the $\{N_{Im}, 3N^-_{amide}\}$ coordination mode. Although the non-equivalence of nitrogen atoms coordinated to Cu(II) ions and the presence of natural abundance mixture of ^{63}Cu and ^{65}Cu, the number of superhyperfine lines (nine) in the $g_\perp$ region of the EPR spectrum is that expected from 4 nitrogen atoms in the plane of coordination ($A_N = 12.8$ G) (Fig. 5(c)).

Among the species obtained for the 7-amino acid peptide 2: CuL, $CuH_{-1}L$, $CuH_{-2}L$, $CuH_{-3}L$ from the 1N to 4N as confirmed by the spectroscopic results reported in Table 4, in the species $CuH_{-4}L$ the deprotonation of the pyrrolic nitrogen takes place. The lack of relevant changes in the spectroscopic parameters supported that there is only a change in the strength of the ligand field in the plane of coordination following deprotonation.

It is interesting to note that the stabilities of the 3N and 4N complexes of peptide 1 are higher than similar complexes of comparable peptides (Table 3) with the exception of the 14-amino acid peptide Cap43. The log K^* values for 3N and 4N complexes of peptide 1 are comparable with those of Cap43. The stability constants of the 4N complexes for peptide 1 and Cap43 are about 1 order of magnitude higher than those of ligands containing one histidine residue within the peptide sequence (Table 3). The imidazole nitrogen acts as the anchoring site for the metal ion, while three amide nitrogens *i.e.*, those of His, Arg and Lys residues complete the coordination in a stepwise mode.[6,13,14]

The behavior of Ac-GK(Ac)GGAK(Ac)RHRK(Ac)V-Am (peptide 3) was the same as the 7-amino acid peptide 2 giving the same spectroscopic results. The EPR and UV-Vis spectra with changing pH are reported in Fig. 5(a) and (d), respectively.

Discussion

This paper reports the results of a study on the interactions of Ni(II) and Cu(II) with the entire tail of the histone H4, the

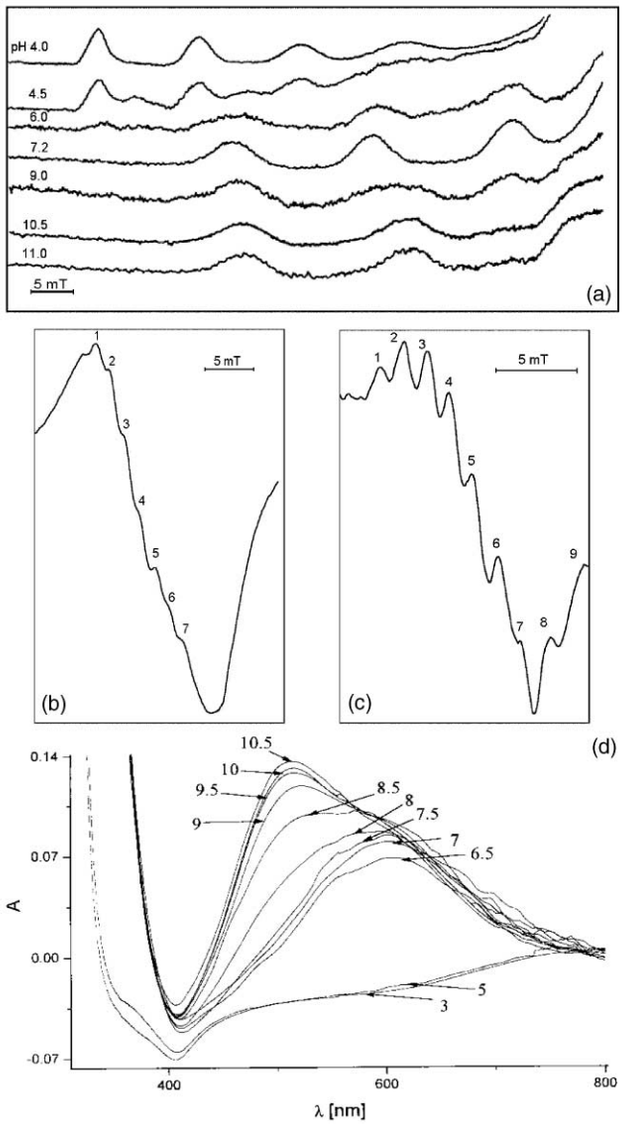

Fig. 5 (a) EPR parallel region of Ac-GK(Ac)GGAK(Ac)RHRK-(Ac)V-Am–Cu(II) [peptide 3–Cu(II)] system with changing pH. (b) EPR perpendicular region of Cu(II)-3N species. (c) EPR perpendicular region of Cu(II)-4N species. (d) UV-Vis spectra of Ac-GK(Ac)GGAK(Ac)RHRK(Ac)V-Am–Cu(II) [peptide 3–Cu(II)] system with changing pH.

22-amino acid peptide Ac-SGRGKGGKGLGKGGAKRHR-KVL-Am (peptide 1) and its short fragments Ac-AK(Ac)-RHRK(Ac)V-Am (peptide 2) and Ac-GK(Ac)GGAK(Ac)-RHRK(Ac)V-Am (peptide 3), in which all the sites for post-translational modification involved in nickel and also in copper toxicity are included.

The results presented above show that peptide 1 binds Ni(II) and Cu(II) through the imidazole nitrogen starting at pH 7 and at pH 3.5, respectively, giving 1N complexes; when pH was raised, both metal ions deprotonated successive peptide nitrogens, forming M–N^- bonds, until MH_2L species (4N complexes) were formed above pH 8 for Ni(II) and pH 6 for Cu(II). The formation of the stable five-membered chelate rings by consecutive nitrogens is the driving force for the coordination process. The stability of the 4N complex of Cu(II) with the 22-amino acid peptide 1 is higher in comparison to that obtained for shorter fragments and it is comparable to that of 14 amino acid peptide Ac-TRSRSHTSEGTRSR-Am, Cap43. The Ni(II) ions with the 22-amino acid fragment (peptide 1) form the 4N complex with similar stability to the shorter fragments of N- and C-blocked peptides containing the histidine residue. The coordination behavior was not significantly affected by the acetylation of lysines.

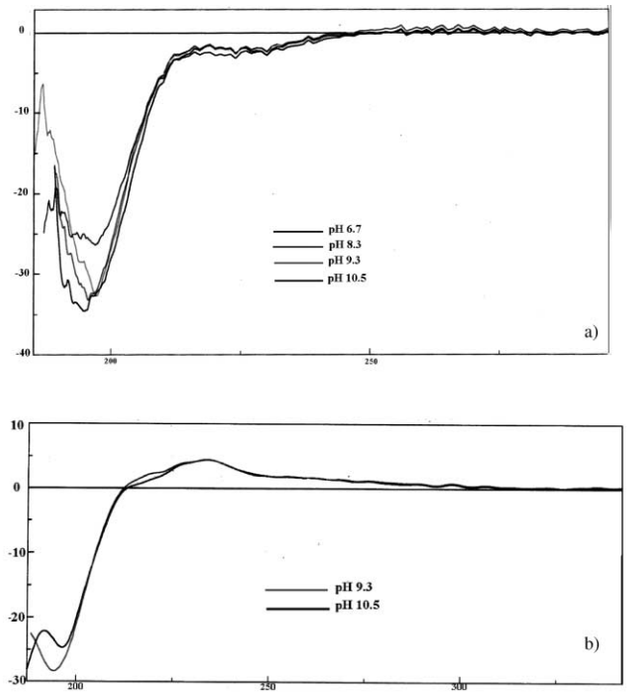

Fig. 6 CD spectra of (a) Ac-SGRGKGGKGLGKGGAKRHRKVL-Am (peptide 1) and (b) Ac-SGRGKGGKGLGKGGAKRHRKVL-Am 4N-Ni(II) species.

In conclusion, histidine 18 close to sites for post-translational modification plays the major role in the coordination behavior of the entire tail of the histone H4.

The pK_a of the N(3) imidazole nitrogen of the histidine residue of the "tail" and of the models investigated are of the same order of magnitude, in the range 5.99–6.13. They are more acidic than other simple peptides, about one order of magnitude more acidic than histidine in Boc-AGGH, Ac-GGGH, Ac-GGH (which have pK_a values of 7.19, 7.21 and 7.18 respectively) where glycine residues instead of arginine or lysine are close to the anchoring site for metal ions.

It is interesting to note that the $pK_a(NH_{im}^+)$ values for our motifs are of the same order of magnitude as that of N-terminal free peptides and where electron-withdrawing groups substitute a hydrogen at the pyrrolic nitrogen.[22] In this case the lower basicity is due both to the electrostatic effect of the positive charge from the NH_3^+-terminus and to the inductive effect of the substituting group. In our case the minor basicity can be associated with the electrostatic effect from the positively charged side chains of R and K, or R, in the peptide ligands.

The log K^* values for the formation, at N(3) of imidazole, of 1N complexes of acetylated peptides are linearly related to the $pK_a(NH_{im}^+)$ in the free peptides.[23] It is to be expected that the labilizing effect of the metal ions on the peptide protons will be strongly influenced by the extent of electron donation by the group acting as the initial coordination locus. Hence, a lower $pK_a(NH_{im}^+)$ value will be associated with a lower degree of electron donation to the metal ion, which will be reflected in a lower value for pK_a(amide) (Table 3). Therefore, the lower basicity of the N(3), the more simple will be the deprotonation, promoted by metal ions, of amide nitrogens resulting in an enhancement of π-electron contribution to the metal–amide nitrogen bond compared to Boc-AGGH or other simple peptides.[24]

This behavior is also reflected in the inverted order of log K^* obtained for 3N and 4N complexes when compared with Boc-AGGH or other simple peptides reported for comparison.

The order for pK_{am} is noteworthy, $pK_{am2} < pK_{am1}$ for copper and $pK_{am3} < pK_{am2}$ for nickel species. This indicates that the deprotonation of the second peptide nitrogen occurs with a

lower pK_a than the first. This behavior is characteristic of the cooperative coordination process found in this peptide coordination mode.[25]

The impact of the secondary peptide structure on the complex stability cannot be excluded.[26] The CD spectra of the fully protonated and deprotonated forms of the "tail" are qualitatively the same, resembling those of unordered peptides. It is interesting to note that, on coordination of the "tail" in a 4N complex with Ni(II), unlike motifs with protected lysines and unlike Cu(II), there was a change in the spectrum with a value of $\Delta\varepsilon$ about 5 mol cm^{-1} dm^{-3} in the region (220–230 nm) dominated by the peptide carbonyl chromophore[27,28] (Fig. 6). This behavior suggests a possible bent structure with organized side-chain orientation promoted by Ni(II).

Although the complexation with Ni(II) at a physiological pH, under our experimental conditions, is not very effective, the formation of a rigid square planar complex may result, somewhat paradoxically, in a higher specificity of Ni(II) to produce a particular conformation of the peptide.[26] The presence of positively charged residues close to the metal binding site in the H4 tail can result in a site-selectivity association of the Ni(II) complexed "tail" with the negatively charged DNA backbone.[29,30] In addition, the hydrophobic environment in the entire protein is expected to enhance metal binding capabilities, due to the multiple non-bonding interactions available, as reported in the literature.[31–33]

In conclusion, the histidine 18 residue can be a primary binding site for Ni(II) ions, therefore the H4 tail can potentially be one of the biologically relevant sites for nickel genotoxicity.

The coordination ability of the entire tail towards Ni(II) is similar to that found previously for the hexapeptide fragment AKRHRK,[14] but the conformation behavior is dependent on the chain length. In fact, Ni(II) coordination to the 22-amino acid peptide 1 induces organized side-chain orientation, unlike Cu(II) and unlike motifs with protected lysines. The data obtained with Ni(II) and Cu(II) metal ions point out an interesting aspect since they seem to show that the sequence of the H4 amino-terminal tail can adopt different conformations depending on the metal ion.

All these facts may be physiologically relevant to the mechanism of nickel carcinogenicity.

Acknowledgements

This work was supported by the Italian MURST, by the Polish State Committee for Scientific Research (KBN 3T09A 105 14) and COST D8 Action (D8/0018/97).

References

1 *IARC Monographs on the Evaluation of Carcinogenic Risks to Humans. Chromium, Nickel and Welding*, IARC, Lyon, France, vol. 49, 1990.
2 M. Costa, *Ann. Rev. Pharmacol. Toxicol.*, 1991, **31**, 321–337.
3 Y. W. Lee, C. B. Klein, B. Kargacin, K. Salnikow, J. Kitahara, K. Dowjat, A. Zhitkovich and M. Costa, *Mol. Cell. Biol.*, 1995, **15**, 2547–2557.
4 K. Salnikow, S. Cosentino, C. Klein and M. Costa, *Mol. Cell. Biol.*, 1994, **14**, 851–858.
5 J. E. Lee, R. B. Ciccarelli and J. K. Wetterhahn, *Biochem.*, 1982, **21**, 771–778.
6 M. A. Zoroddu, T. Kowalik-Jankowska, H. Kozłowski, H. Molinari, K. Salnikow, L. Broday and M. Costa, *Biochim. Biophys. Acta*, 2000, **1475**, 163–168.
7 L. Broday, W. Peng, M. H. Kuo, K. Salnikow, M. A. Zoroddu and M. Costa, *Cancer Res.*, 2000, **60**, 238–241.
8 M. Grunstein, *Nature*, 1997, **389**, 349–352.
9 J. Meienhofer, M. Waki, E. P. Heimer, T. J. Lambros, R. C. Makofske and C. D. Chang, *Int. J. Pept. Protein Res.*, 1979, **13**, 35–42.
10 H. Irving, M. G. Miles and L. D. Pettit, *Anal. Chim. Acta*, 1967, **38**, 475–488.
11 P. Gans, A. Sabatini and A. Vacca, *J. Chem. Soc., Dalton Trans.*, 1985, 1195–1199.
12 G. Bodenhausen, R. L. Vold and R. R. Vold, *J. Magn. Res.*, 1980, **37**, 93–106.
13 T. Kowalik-Jankowska, M. Ruta-Dolejsz, K. Wiśniewska, L. Łankiewicz and H. Kozłowski, *J. Chem. Soc., Dalton Trans.*, 2000, 4511–4519.
14 T. Kowalik-Jankowska, M. Ruta-Dolejsz, K. Wiśniewska and L. Łankiewicz, *J. Inorg. Biochem.*, 2001, **86**, 535–545.
15 W. Bal, H. Kozłowski, R. Robbins and L. D. Pettit, *Inorg. Chim. Acta*, 1995, **231**, 7–12.
16 M. A. Zoroddu, T. Kowalik-Jankowska, H. Kozłowski, K. Salnikow and M. Costa, *J. Inorg. Biochem.*, 2001, **84**, 47–54.
17 W. Bal, M. Dyba and H. Kozłowski, *Acta Biochim. Pol.*, 1997, **44**, 467–470.
18 W. Bal, M. Dyba, F. Kasprzykowski, H. Kozłowski, R. Latajka, L. Łankiewicz, Z. Mackiewicz and L. D. Pettit, *Inorg. Chim. Acta*, 1998, **283**, 1–11.
19 L. D. Pettit, J. E. Gregor and H. Kozłowski, in *Perspectives on Bioinorganic Chemistry*, ed. R. W. Hay, J. R. Dilworth and K. B. Nolan, JAI Press, London, 1991, vol. 1, pp. 1–41.
20 W. Bal, J. Lukszo, J. K. Bialkowski and K. S. Kasprzak, *Chem. Res. Toxicol.*, 1998, **11**, 1014–1023.
21 W. Bal, J. Lukszo and K. S. Kasprzak, *Chem. Res. Toxicol.*, 1996, **9**, 535–540.
22 L. Pettit, S. Pyburn, W. Bal, H. Kozłowski and M. Bataille, *J. Chem. Soc., Dalton Trans.*, 1990, 3565–3570.
23 G. F. Bryce, R. W. Roeske and F. Gurd, *J. Biol. Chem.*, 1965, **240**, 3837–3846.
24 P. Młynarz, N. Gaggelli, J. Panek, M. Stasiak, G. Valensin, T. Kowalik-Jankowska, M. T. Leplawy, Z. Latajka and H. Kozłowski, *J. Chem. Soc., Dalton Trans.*, 2000, 1033.
25 H. Sigel and R. B. Martin, *Chem. Rev.*, 1982, **82**, 393–394.
26 H. Kozłowski, W. Bal, M. Dyba and T. Kowalik-Jankowska, *Coord. Chem. Rev.*, 1999, **184**, 319–346.
27 W. Bal, H. Kozłowski, G. Kupryszewski, Z. Mackiewicz, L. Pettit and R. Robbins, *J. Inorg. Biochem.*, 1993, **52**, 79–87.
28 R. W. Woody, in *The Peptides*, ed. V. Hruby, Academic Press, New York, 1985, vol. 7.
29 D. F. Shullenberg, P. Eason and E. C. Long, *J. Am. Chem. Soc.*, 1993, **115**, 11038–11039.
30 Q. Liang, P. D. Eason and E. C. Long, *J. Am. Chem. Soc.*, 1995, **117**, 9625–9631.
31 W. Bal, G. N. Chmurny, B. D. Hilton, P. J. Sadler and A. Tucker, *J. Am. Chem. Soc.*, 1996, **118**, 4727–4728.
32 M. M. Yamashita, L. Wesson, G. Eisenman and D. Eisenberg, *Proc. Natl. Acad. Sci. USA*, 1990, **87**, 5648–5652.
33 L. Regan, *Annu. Rev. Biophys. Biomol. Struct.*, 1993, **22**, 257–281.